ISSN 2706-655X Vol.3, Issue 5: 1-9, DOI: 10.25236/IJFET.2021.030501

Research on Backscattering Model with Row Structure on Farmland

Fan Yu[1,2a*], Hao-Nan Wang[1,2b] and Chengming Zhang[3,c]

[1]*Lanzhou Institute of drought meteorology, Lanzhou, 730000, China*
[2]*School of Geomatics and Urban Spatial Informatics, Beijing University of Civl Engineering and Architecture, Beijing, 100044, China*
[3]*Shandong Agricultural University, College of Information Science and Engineering, Shandong 271018, China*
[a]*yufan@bucea.edu.cn,* [b]*hn_w1997@163.com,* [c]*Chming@sdau.eud.cn*
**corresponding author e-mail: yufan@bucea.edu.cn*

Abstract: *The row structure in agricultural surface is key for effectively explaining SAR backscattering coefficient. The row structure is described by a mathematical method at first in this research, and a surface scattering model, called AAIEM (Agriculture Advanced Integral Equation Model) is presented in the paper. In the AAIEM, the row structure is assumed to be the combining of the periodic row surface and small-scale random rough surface over the row surface. Then, the polarimetric deflection angle is correct and the backscattering coefficient is calculated by derived AAIEM. The model is validated by AIEM and field measurements, the results show that comparing to AIEM, the AAIEM can better simulate the backscattering in the row structure surface, and it is more suitable for C/L band SAR signal. Our research provide theoretical foundation and technical support for development of precision agriculture in future.*

Keywords: *agricultural surface with row structure, backscattering, AAIEM, polarimetric deflection angle*

1. Introduction

Microwave remote sensing has been paid more and more attention because of the long wavelength, the ability to penetrate clouds and fog and the characteristic that can not be affected by weather. However, the scattering model of random surface is always a hot and difficult point in microwave remote sensing research. The theoretical model of microwave scattering is based on the strict electromagnetic theory, and the relationship between the backscattering coefficients and the physical and geometric parameters of the surface is established through mathematical derivation [1]. Due to the complex shape of the natural surface, it is difficult to obtain the exact analytical solution of electromagnetic wave scattering by solving Maxwell equation directly, so the approximate solution can only be obtained by hypothesis and approximation under certain restriction conditions. Such approximate models mainly include Physical Optics Model (POM), Geometric Optics Model (GOM), Small Perturbation Model (SPM) [2], etc. These approximate models have a certain scope of application. Simply speaking, both POM and GOM are obtained by Kirchhoff approximation (KA), in which the POM is suitable for medium roughness, while the GOM is suitable for larger roughness. The SPM is suitable for smooth surface with small roughness. At present, the most widely used surface scattering model in remote sensing is the Integral Equation Model(IEM)[3], which can reproduce the real surface backscattering in a wide range of surface roughness and is widely used in the simulation and analysis of microwave surface scattering and radiation. Many scholars have improved the mathematical simplification and physical approximation used by IEM, and developed a more accurate AIEM model [4-5]. This model modifies the limitation of Green function and Fresnel reflection coefficient in the original IEM model, and introduces Transition Model to solve the uncertainty of whether to adopt the Fresnel reflection coefficient with the incident angle as the parameter or the Fresnel approximation with the observation angle as the parameter under different roughness conditions.

However, a very common case in agriculture is the anisotropy of scattering caused by the ridge structure of the field. Using common surface scattering models, such as KA, SPM, AIEM, etc., the

ISSN 2706-655X Vol.3, Issue 5: 1-9, DOI: 10.25236/IJFET.2021.030501

calculation error is very large for farmland with obvious ridge, because these models are mainly used to calculate random rough soils that are isotropic or isotropic in two vertical directions. Because of the existence of ridges, not only the incident angles of ridges at different positions in pixels are different, but also the horizontal and vertical polarization directions and the radar reference directions are different, resulting in orientation angles. As a result, the simulation results of the theoretical model deviate from the actual situation.

At present, there are some literatures on the scattering theory of ridge farmland [6-8]. Ulaby et al [9]. Considered that the periodic ridge structure had an important influence on the backscattering coefficient of soil, and neglecting this effect would lead to larger errors. Promes et al. [10] used sine function to approximate the periodic ridge structure of farmland and achieved good results, and meanwhile, they also analyzed the relationship between the ridge structure parameters and emissivity at different incident angles. Beaudoin et al. [11] proposed a concept of multiple roughness, which divided farmland into large-scale periodic surface, mesoscale periodic surface and small-scale random surface, and then combined them to express the roughness of farmland by using complex mathematical relations. The C-band SAR data were used to verify that the multi-roughness could better express the ridge structure of farmland. When the incident angle was less than 50 °, the error between the simulation results of the multi-roughness model and the measured value was within 2dB. Zheng Xingming et al. [12] also discussed the influence of ridge structure on inversion of soil moisture by passive microwave remote sensing, and pointed out that the soil moisture inversion errors caused by surface emissivity changes caused by ridge mostly exceeded 0.04.

Most of the above studies focus on the emissivity model of passive microwave, and do not consider the effect of orientation angle, and some scholars pay attention to the expression of farmland roughness with ridge structure, and have not established a model suitable for ridge structure. Based on this consideration, a surface scattering model for ridge-structured farmland is proposed. The ridge is regarded as the superposition of periodic ridge surface and small-scale random rough surface on ridge surface. Based on the simulation of backscattering coefficient by AIEM, an AAIEM (Agriculture AIEM) suitable for ridge-structured farmland is developed. Then the AAIEM method is validated by AIEM model and measured data.

2. Study on Back Scattering Model of Ridge-Structured Farmland

2.1 Description of Ridge Structure

The geometric relationship between ridge and radar incident wave is shown in Fig.1. The angle between the direction of the radar flight and the direction of the ridge is the arbitrary angle as shown by the red line. The unit vector of incident direction is expressed by Î. Because of the non-isotropic surface, i.e. the ridge and the incident direction can form a certain angle, it is impossible to assume that the incident plane is in X-O-Z, and the azimuth angle φi is not always zero, then there is

$$\hat{I} = \cos\varphi_i \sin\vartheta_i \hat{x} + \sin\varphi_i \sin\vartheta_i \hat{y} - \cos\vartheta_i \hat{z} \tag{1}$$

$\hat{i}$ and $\hat{n}$ are the unit vector and normal vector of incident wave respectively. It should be noted that according to the definition, the range of θl and ϑi is 0-90°, and the range of variation of φi is 0-90 °.

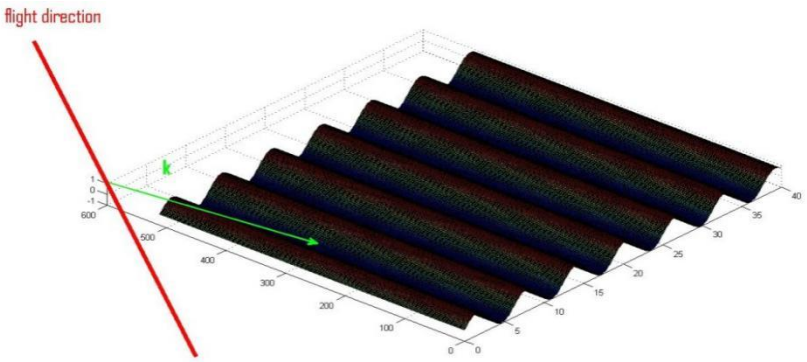

Fig.1 Geometry relationship of ridge and radar

ISSN 2706-655X Vol.3, Issue 5: 1-9, DOI: 10.25236/IJFET.2021.030501

The ridge parameters, such as ridge height and width inclination, can be easily measured in large-scale mechanically cultivated farmland. Therefore, it is not difficult to obtain a function describing ridge elevation. If the elevation function of ridge surface is set to zp(x,y) and the height of small-scale random roughness of ridge surface is set to $z_s(x, y)$, the elevation of any point can be expressed as follows:

$$z = z_p + z_s \tag{2}$$

Let $z_s(x, y)$ be:

$$z_s = \frac{z_n}{n_z} \tag{3}$$

nz is the z component of the unit normal vector, and zn is the zero-mean Gaussian random variable assumed by us in the traditional isotropic random rough soil, which satisfies some correlation function, such as exponential function:

$$\langle z_n(x, y) z_n(x', y') \rangle = h_{RMS}^2 \exp(-\frac{r}{Lc}) \tag{4}$$

Or gaussian function:

$$\langle z_n(x, y) z_n(x', y') \rangle = h_{RMS}^2 \exp(-\frac{r^2}{Lc^2}) \tag{5}$$

2.2 Backscattering Model of Farmland Based on Ridge Effect

In modeling, assuming that a pixel package covers multiple periods and the effect of its non-integer periodic part can be neglected, then the integral can be carried out for the small surface elements in a complete ridge P.

$$\sigma_{qp}^0(\vartheta_l) = \frac{1}{A\cos\vartheta_l} \int_P dS \cos\vartheta_l \tilde{\sigma}_{qpl}^0(\vartheta_l) U(90 - \vartheta_l) \tag{6}$$

Where ϑl is the local incident angle and U(ϑl) is a step function, which is used to consider the shadow effect. Since only the case of incoherent superposition is considered here, the shadow surface is considered as the part that can't be illuminated. $\tilde{\sigma}_{qpl}^0(\vartheta_l)$ is a local normalized backscattering cross section. The local incident angle can be calculated by the following formula:

$$\vartheta_l = \arccos(\hat{s} \cdot \hat{n}) \tag{7}$$

According to the reciprocity principle, the covariance matrix C3 of backscattering is simple in form, with three rows and three columns. Therefore, the expression of $\tilde{\sigma}_{qpl}^0(\vartheta_l)$ can be obtained completely by the orientation angle compensation formula in reference [13], and θl is replaced by -θl, and then the following can be obtained:

$$\begin{aligned} \tilde{\sigma}_{hhl}^0(\vartheta_l) = & \cos^4(\theta_l)\sigma_{hh}^0(\vartheta_l) + 2\cos^2(\theta_l)\sin(2\theta_l)\mathrm{Re}\langle\sigma_{hhhv}^0(\vartheta_l)\rangle \\ & + \frac{1}{2}\sin^2(2\theta_l)\mathrm{Re}\langle\sigma_{hhvv}^0(\vartheta_l)\rangle + \sin^2(2\theta_l)\sigma_{hv}^0(\vartheta_l) \\ & + 2\sin^2(\theta_l)\sin(2\theta_l)\mathrm{Re}\langle\sigma_{hvvv}^0(\vartheta_l)\rangle + \sin^4(\theta_l)\,\sigma_{vv}^0(\vartheta_l) \end{aligned} \tag{8}$$

ISSN 2706-655X Vol.3, Issue 5: 1-9, DOI: 10.25236/IJFET.2021.030501

$$\begin{aligned}\tilde{\sigma}^0_{vvl}(\vartheta_l)=&\sin^4(\theta_l)\sigma^0_{hh}-2\sin(2\theta_l)\sin^2(\theta_l)\mathrm{Re}\left\langle\sigma^0_{hhhv}(\vartheta_l)\right\rangle\\&+\frac{1}{2}\sin^2(2\theta_l)\mathrm{Re}\left\langle\sigma^0_{hhvv}(\vartheta_l)\right\rangle+\sin^2(2\theta_l)\sigma^0_{hv}(\vartheta_l)\\&+2\cos^2(\theta_l)\sin(2\theta_l)\mathrm{Re}\left\langle\sigma^0_{hvvv}(\vartheta_l)\right\rangle+\cos^4(\theta_l)\sigma^0_{vv}(\vartheta_l)\end{aligned}\tag{9}$$

According to the principle of Reflection Symmetry of natural targets, there is:

$$\sigma^0_{hhhv}(\vartheta_l)=\frac{1}{\sqrt{2}}\left\langle S_{hh}S^*_{hv}\right\rangle=0,\ \sigma^0_{hvvv}(\vartheta_l)=\frac{1}{\sqrt{2}}\left\langle S_{hv}S^*_{vv}\right\rangle=0\tag{10}$$

Then the Formula (8) and Formula (9) can be written as follows:

$$\begin{aligned}\tilde{\sigma}^0_{hhl}(\vartheta_l)=&\cos^4(\theta_l)\sigma^0_{hh}(\vartheta_l)+\frac{1}{2}\sin^2(2\theta_l)\mathrm{Re}\left\langle\sigma^0_{hhvv}(\vartheta_l)\right\rangle\\&+\sin^2(2\theta_l)\sigma^0_{hv}(\vartheta_l)+\sin^4(\theta_l)\,\sigma^0_{vv}(\vartheta_l)\end{aligned}\tag{11}$$

$$\begin{aligned}\tilde{\sigma}^0_{vvl}(\vartheta_l)=&\sin^4(\theta_l)\sigma^0_{hh}+\frac{1}{2}\sin^2(2\theta_l)\mathrm{Re}\left\langle\sigma^0_{hhvv}(\vartheta_l)\right\rangle\\&+\sin^2(2\theta_l)\sigma^0_{hv}(\vartheta_l)+\cos^4(\theta_l)\sigma^0_{vv}(\vartheta_l)\end{aligned}\tag{12}$$

The scattering coefficients on the right side of Formula (11) and Formula (12) can be calculated by the current general scattering model. In this chapter, AIEM, which is considered to be the most accurate approximate model in remote sensing, is used to calculate.

Without losing generality, let the coordinate of any point be set as (x,y,z). In calculation, the integral area is limited to a periodic surface element perpendicular to the ridge direction, assuming that the ridge direction is y direction, and the ridge height with periodic variation varies along the x direction. Therefore, the double integral in Formula (6) can be replaced by a single integral, i.e.

$$\sigma^0_{qp}\left(\vartheta\right)=\frac{1}{P\cos\vartheta}\int dx\sqrt{1+\left(\frac{dz_l}{dx}\right)^2}\cos\vartheta_l\tilde{\sigma}^0_{qpl}(\vartheta_l)U\left(90-\vartheta_l\right)\tag{13}$$

Then the coordinate of its normal vector is:

$$\begin{aligned}\hat{n}=&\frac{1}{\sqrt{\left(\frac{\partial z_l}{\partial x}\right)^2+\left(\frac{\partial z_l}{\partial y}\right)^2+1}}\left(-\frac{\partial z_l}{\partial x},-\frac{\partial z_l}{\partial y},1\right)\\=&\frac{1}{\sqrt{\left(\frac{dz_l}{dx}\right)^2+1}}\left(-\frac{dz_l}{dx},0,1\right)=(n_x,0,n_z)\end{aligned}\tag{14}$$

2.3 Processing of Orientation Angle

The orientation angle is defined as the angle between the reference horizontal polarization vector and the local horizontal polarization vector. Fig.2 shows a geometric diagram of the orientation angle. Let X-Y-Z be the coordinate system satisfying the right-handed helix and X-O-Z plane be the incident plane. The reference horizontal polarization vector is parallel to the Y axis, that is, $\hat{H}_0$ is parallel to the X-O-Y plane. $\hat{V}_0$ is the reference vertical polarization direction. $\overline{k}$ is a wavenumber vector. $\hat{H}_0,\hat{V}_0$, and $\overline{k}$ satisfy the right-handed helix. More generally, however, on an inclined surface, local $\hat{H}_l$ is no longer parallel to the XOY plane. Correspondingly, all polarization responses deviate from the theoretical values due to the slope, such as the prediction of AIEM model. The formula for calculating the local horizontal polarization vector is as follows:

ISSN 2706-655X Vol.3, Issue 5: 1-9, DOI: 10.25236/IJFET.2021.030501

$$\hat{H}_l = \frac{\hat{N} \times \hat{k}}{\left| \hat{N} \times \hat{k} \right|} \tag{15}$$

The orientation angle θl can be calculated according to the method of calculating orientation angle by DEM in reference [14]. The difference is that the azimuth angle of incident direction in this paper is not necessarily zero. θl and radar incidence direction are related to the shape of ridge direction. When the reference coordinate system is used, the X-O-Z plane needs to be transferred to the incident plane, and the z-axis is parallel to the incident direction. The angle φi needs to be rotated around the z-axis first and then the angle ϑi is rotated around the new y-axis. Therefore, the coordinate of the local normal vector $\hat{n}$ in the new coordinate system is:

$$\begin{bmatrix} n_x' \\ n_y' \\ n_z' \end{bmatrix} = R_y(\vartheta_i) R_z(\varphi_i) \begin{bmatrix} n_x \\ n_y \\ n_z \end{bmatrix} \tag{16}$$

Where

$$R_z(\varphi_i) = \begin{bmatrix} \cos\varphi_i & \sin\varphi_i & 0 \\ -\sin\varphi_i & \cos\varphi_i & 0 \\ 0 & 0 & 1 \end{bmatrix}, \quad R_y(\vartheta_i) = \begin{bmatrix} \cos\vartheta_i & 0 & -\sin\vartheta_i \\ 0 & 1 & 0 \\ \sin\vartheta_i & 0 & \cos\vartheta_i \end{bmatrix} \tag{17}$$

Then the coordinate system is rotated around the direction of the incident wave, i.e. the new z-axis with an angle of -θl, and then $\hat{n}$ is in the local incident plane, and its y-coordinate is 0, and then there is:

$$\begin{bmatrix} n_x'' \\ n_y'' \\ n_z'' \end{bmatrix} = R_z(-\theta_l) R_y(\vartheta_i) R_z(\varphi_i) \begin{bmatrix} n_x \\ n_y \\ n_z \end{bmatrix} \tag{18}$$

From ny"=0, it can be seen that:

$$\tan\theta_l = \frac{n_x \sin\varphi_i}{n_x \cos\varphi_i \cos\vartheta_i - n_z \sin\vartheta_i} \tag{19}$$

As can be seen from Formula (19), there are two special cases.

(1)When the incident wave is perpendicular to the ridge direction, θl =0o, that is, there is no orientation angle.

(2)When the denominator in Formula (19) is 0, the reference coordinate system and the local horizontal polarization vector are calculated directly. Considering nxcosφicosϑi=nzsin ϑi and the dot product of the two is zero, therefore θl =90o.

3. Model Verification

3.1 AIEM Model Verification

In this paper, taking the most common trapezoidal ridge as an example, the backscattering coefficients of farmland with ridge effect calculated by AAIEM and AIEM are compared, and the difference of scattering characteristics between farmland with ridge and isotropic random rough soil is compared. The inclination angle of ridge is fixed at 45 °, and the projection length ratio of hypotenuse to horizontal side in x direction is 1:1, as shown in Fig.3. In the case of trapezoidal ridge, since AAIEM calculates the normalized backscattering cross section, when the parameters of ridge shape are given, the scattering cross section is independent of the absolute size.

ISSN 2706-655X Vol.3, Issue 5: 1-9, DOI: 10.25236/IJFET.2021.030501

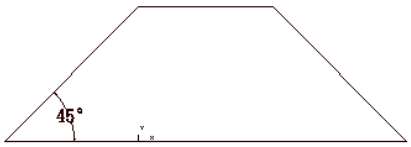

Fig.2 Schematic diagram of trapezoid ridge

In Fig.3, the backscattering coefficients of trapezoidal ridge farmland in L band are simulated with AAIEM and AIEM under different parameters. The roughness parameters are the values after removing the ridge surface. The dielectric constant in the figure is set to $\varepsilon_r=6+0.5i$, and the surface correlation length is Lc=0.5λ. Fig.3(a)-(c) are moderately rough, and hRMS=0.1λ; Fig.3(d)-(f) are relatively smooth, and hRMS=0.05λ; Fig.3(e)-(g) are particularly smooth, and hRMS=0.025λ. For a group of graphs with the same roughness, the azimuth angle φi is 0°, 45° and 90°, respectively.

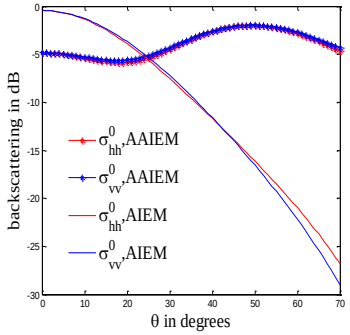

(a) $\varphi_i = 0°$, $h_{RMS}=0.1\lambda$, $L_c=0.5\lambda$

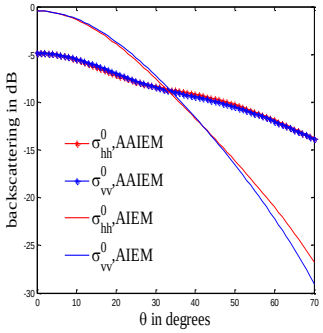

(b) $\varphi_i = 45°$, $h_{RMS}=0.1\lambda$, $L_c=0.5\lambda$

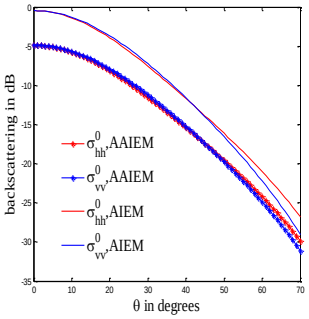

(c) $\varphi_i = 90°$, $h_{RMS}=0.1\lambda$, $L_c=0.5\lambda$

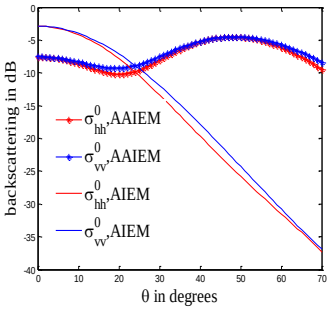

(d) $\varphi_i = 0°$, $h_{RMS}=0.05\lambda$, $L_c=0.5\lambda$

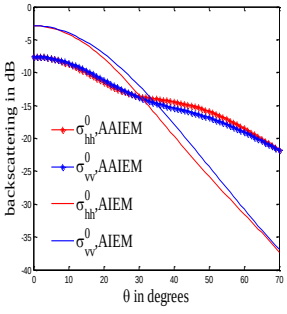

(e) $\varphi_i = 45°$, $h_{RMS}=0.05\lambda$, $L_c=0.5\lambda$

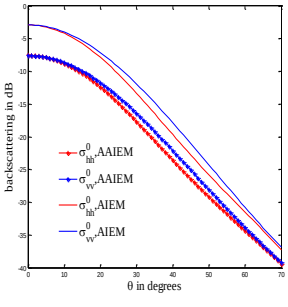

(f) $\varphi_i = 90°$, $h_{RMS}=0.05\lambda$, $L_c=0.5\lambda$

ISSN 2706-655X Vol.3, Issue 5: 1-9, DOI: 10.25236/IJFET.2021.030501

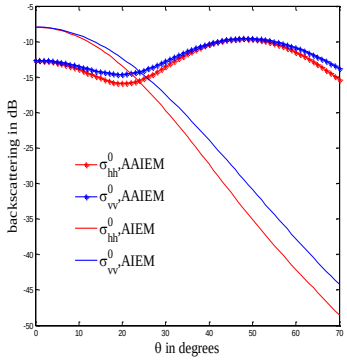

(g) $\varphi_i = 0°$, $h_{RMS}=0.025\lambda$, $L_c=0.5\lambda$

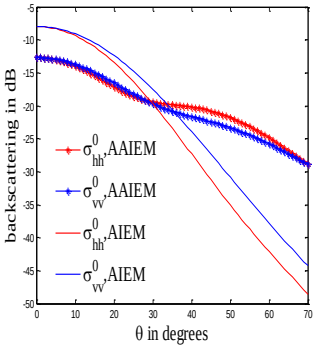

(h) $\varphi_i = 45°$, $h_{RMS}=0.025\lambda$, $L_c=0.5\lambda$

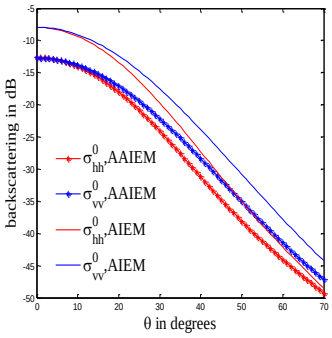

(i) $\varphi_i = 90°$, $h_{RMS}=0.025\lambda$, $L_c=0.5\lambda$

Fig.3 Comparing of bare soil scattering coefficients simulated by AAIEM and AIEM from trapezoidal fields

It can be seen that the variation trend of AAIEM and AIEM simulation results with roughness is the same in magnitude. However, there are obvious differences between AAIEM and AIEM with respect to the change of incident angle, which is very obvious with respect to the change of relative azimuth angle. When φi=0o, that is, the angle between the azimuth direction of incident wave and ridge direction is 90 °, the change difference between AAIEM and AIEM with incident angle is the greatest. When φi=90o, that is, the azimuth direction of incident wave and ridge direction are parallel, the change trend of both with incident angle is the closest. Another characteristic of backscattering coefficient of trapezoidal ridge is that when φi=0o, a peak will appear near the incident angle ϑi=45o, which is mainly caused by the inclination of the ridge at 45 °. When ϑi=45o and φi=0o, a vertical incidence will occur at an inclined edge. At this time, the backscattering direction coincides with the forward scattering direction, and the scattering is the strongest, which also contributes to the total scattering coefficient.

4. Conclusions

In this paper, based on AIEM, a computational model AAIEM for backscattering coefficient of soil considering ridge effect of farmland is proposed. The model decomposes the ridge structure into the superposition of periodic ridge surface and small-scale random rough surface of ridge surface. The former is determined, while the latter is random, accumulating the contribution of local scattering at the intensity level. At the same time, the model takes into account the changes of local incident angle and local polarization direction caused by "ridge", and the calculation of surface backscattering can be realized by using AIEM when the surface soil dielectric constant, roughness parameters and the angle between radar incidence direction and ridge direction are known. The AAIEM model is validated by using AIEM model and measured data. The results show that:

(1) In the scattering simulation of trapezoidal farmland, the backscattering coefficients of AAIEM and AIEM vary with the roughness, and the magnitude of change is in the same order of magnitude. However, the influence of the change of incident angle and azimuth angle on them is different. When

ISSN 2706-655X Vol.3, Issue 5: 1-9, DOI: 10.25236/IJFET.2021.030501

the azimuth angle φi=90o, the backscattering coefficients simulated by AAIEM and AIEM have an approximate trend, which decreases sharply with the increase of incident angle. However, when φi=0o or φi=45o, the results of the two simulations differ significantly. With the increase of incident angle, the results of AIEM simulation decrease significantly, while the results of AAIEM show irregular changes (φi=0o) or small decreases (φi=45o).

(2) The simulation results of AAIEM are close to the measured data on the ground in C/L band, with a small error, while AIEM model has a large error, indicating that the model in this paper is accurate and effective for ridge farmland, and is more suitable for simulation of backscattering coefficient of ridge farmland in C/L band.

(3) The simulation results of AAIEM in P band are quite different from the measured data on the ground. This may be because, on the one hand, the penetration depth of P band is relatively deep, which does not correspond well with the measured soil moisture of 0-10cm, and on the other hand, the ridge height in this experiment is relatively small relative to the wavelength, resulting in no obvious macroscopic topographic effect of the ridge structure, making the model no longer applicable.

In the future research of precision agriculture, there may be a wide demand for scattering simulation of large-scale cultivated farmland and inversion of soil moisture content. In addition, after the emergence of mechanized agriculture on a large scale in China, this demand will become very urgent. Therefore, the AAIEM model proposed in this paper will provide a basis for these developments.

Acknowledgments

This work is jointly supported by Drought Meteorological Science Research Foundation (IAM201902) and Research on quality detection method of land cover classification based on depth confidence neural network (201901)

References

[1] Ulaby FT, Moore R K, Fung A K. Microwave remote sensing. Volume Ⅱ: Radar Remote Sensing and surface Scattering and Emission Theory. Addison-Wesley Publishing Company, 1982.

[2] Wetzel L B. A model for sea backscatter intermittency at extremely grazing angles[J], Radio Science, 1977, 5:749-756

[3] Fung A K, Backscattering from a randomly rough dielectric surface [J]. IEEE Trans. Geosci. Remote Sensing, 1992, 30 :356-369

[4] Chen K S, Wu T D, Leuing T, et al. Emission of rough surfaces calculated by the integral equation method with comparison to Three-Dimensional Moment Method simulations [J]. IEEE Transaction on Geoscience and Remote Sensing, 2003, 41(1): 90-101.

[5] Wu T D, Chen K S, Shi J C. A study of an AIEM model for bistatic scattering from randomly rough surfaces [J]. IEEE Transactions on Geoscience and Remote Sensing, 2008, 49: 2584-2598.

[6] W. Liu, L. Guo, and A. Wang, "A polarimetric scattering research of ocean surface based on the matrix of scattering facet." pp. 1687-1690.

[7] H. Stephen, and D. G. Long, "Analysis of scatterometer observations of Saharan ergs using a simple rough facet model." pp. 1534-1537 vol. 3.

[8] M. Zhang, H. Chen, and H. C. Yin, "Facet-Based Investigation on EM Scattering From Electrically Large Sea Surface With Two-Scale Profiles: Theoretical Model," Geoscience and Remote Sensing, IEEE Transactions on, (2011), no. 99, pp. 1-9.

[9] Ulaby F T, Kouyate F, Fung A K and Sieber A J. 1982. A backscatter model for a randomly perturbed periodic surface. IEEE Transactions on Geoscience and Remote Sensing, GE-20(4): 518–528 [DOI: 10.1109/TGRS.1982.350420]

[10] Promes P M, Jackson T J and O'Neill P E. 1988. Significance of agricultural row structure on the microwave emissivity of Soils. IEEE Transactions on Geoscience and Remote Sensing, 26(5): 580–589 [DOI: 10.1109/36.7683]

[11] Beaudoin A, Toan T L, Gwin Q H. SAR Observations and Modeling of the C-Band Backscatter Variability Due to Multiscale Geometry and Soil Moisture. IEEE Transactions on Geoscience and Remote Sensing. 1990, 28(5): 886-895

[12] Zheng Xing Ming, Zhao Kai, Zhang Shu Wen. Effect of ridge structure on soil moisture retrieval by passive microwave remote sensing. Journal of Remote Sensing, 2012,16 (6): 1320-1330

ISSN 2706-655X Vol.3, Issue 5: 1-9, DOI: 10.25236/IJFET.2021.030501

[13] Xinyi Shen, Yang Hong, Qiming Qin, Weilin Yuan, Sheng Chen, Trevor Grout, and Shaohua Zhao, (2011) Orientation Angle Calibration for Bare Soil Moisture Estimation Using Fully Polarimetric SAR Data. IEEE Transactions on Geoscience and Remote Sensing.vol. 49(12) pp.4987-4996.

[14] J. S. Lee, D. L. Schuler, and T. L. Ainsworth, "Polarimetric SAR data compensation for terrain azimuth slope variation," IEEE Transactions on Geoscience and Remote Sensing, (2000), vol. 38, no. 5, pp. 2153-2163.